On the Mismatch of Emission Requirements for CW Interference Against OFDM Systems

Karina Mariana Fors, Kia Cecilia Wiklundh, and Peter F. Stenumgaard

***Abstract*—Several modern digital wireless services, such as long-term evolution, relies on orthogonal frequency division multiplex (OFDM). OFDM is in general vulnerable to narrow-band interference such as continuous wave (CW). Earlier publications have indicated that this vulnerability is dependent on where in the OFDM-receiving frequency band the CW interference appears. In this paper, this frequency dependence is rigorously investigated and explained with both theoretical and numerical results. It is shown that by varying the CW frequency within a single OFDM subchannel, very large variations (several magnitudes, e.g., 10^4 times) corresponding to bit error probability are obtained. This dependence in vulnerability is not considered in present radiated emission standards, and therefore a suggestion about how this could be handled is also presented.**

***Index Terms*—Continuous wave (CW) interference, emission requirements, narrowband interference, orthogonal frequency division multiplex (OFDM).**

I. Introduction

ORTHOGONAL frequency division multiplex (OFDM) is used in several modern wireless services. Examples are the mobile technologies 4G [long-term evolution (LTE)] and coming 5G, the wireless local area network standard IEEE 802.11, digital audio broadcasting, and digital video broadcasting. Furthermore, 4G is under consideration in several countries as a replacement technology for the current terrestrial trunked radio based systems for emergency and crisis communications. The reason for the growing use of OFDM can be found from the need of high data rate applications. To achieve high communication data rates, intersymbol interference (ISI) is an inevitable problem due to the channel delay spread for single carrier systems. To handle this problem, OFDM is a solution. By dividing the bandwidth into a multiple number of narrow-banded signals, so-called multicarriers, the ISI can be reduced [1]. With this operation, the high-speed data stream is divided into several parallel lower rate data streams prior the transmission. OFDM is a multicarrier transmission technique, where the subcarriers are overlapping each other in a controlled manner so that the subcarriers become orthogonal and do not interfere with each other. Another advantage of the OFDM technique is that it can easily be implemented by using fast Fourier transform (FFT). A commonly known drawback with the OFDM technique is that a large peak-to-average power ratio may appear. This may reduce the efficiency of the used power amplifier in the system.

Another drawback is its large vulnerability to narrowband interference such as continuous wave (CW). A few previous publications [2], [3] have indicated that this vulnerability is also dependent on the exact frequency. However, a rigorous analysis that explains the phenomenon is lacking. In this paper, this frequency dependence is, therefore, thoroughly investigated and explained. The investigation is based on a theoretical analysis and simulations of a communication system subjected to interfering CW signals. It is shown that this dependence can cause large variations in communication performance due to where in frequency the interference is located. Furthermore, we show that the power of a CW interference within a single subcarrier must be about 18 dB lower than the corresponding power of additive white Gaussian noise (AWGN) to not exceed a bit error probability (BEP) of 10^5. Thus, an OFDM system is considerably more sensitive to a CW interference than to AWGN. This is an important fact to be considered in system design and when maximum interference limits are to be determined for different system applications. Moreover, since the interference type (CW or AWGN) and the frequency dependence are not considered in previous emission standards, further work is needed to develop a strategy for how to handle this mismatch in vulnerability analyses.

In [4], a possible method of estimating the interference impact from present emission standard levels has been proposed but this vulnerability of OFDM systems is not included in that work. Furthermore, this vulnerability is important to consider with respect to protection against intentional electromagnetic interference, since that threat has become real in recent years [5]–[7].

The paper is organized as follows. In Section II, we present the OFDM system model as well as the interference signal model for the analyses. In Section III, the results from the vulnerability analysis are shown for an OFDM system with LTE-like radio parameters and different interference assumptions. In Section IV, a discussion is done over the possibility to consider this varying vulnerability and how emission measurements may be developed so that the results could be used to consider this large variation in interference impact. The paper is concluded in Section V.

Manuscript received July 7, 2017; revised October 9, 2017; accepted November 2, 2017. Date of publication December 26, 2017; date of current version May 29, 2018. *(Corresponding author: Kia Cecilia Wiklundh.)*

The authors are with the Swedish Defence Research Agency, Linköping SE-58111, Sweden (e-mail: karina.fors@foi.se; kia.wiklundh@foi.se; peter.stenumgaard@foi.se).

Digital Object Identifier 10.1109/TEMC.2017.2775649

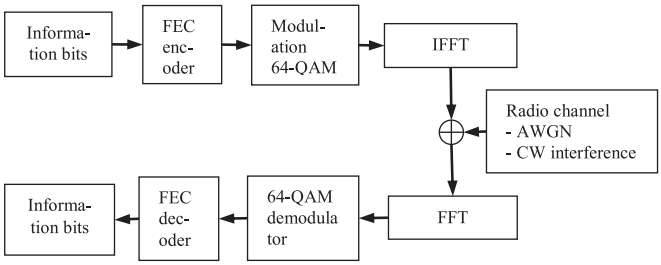

Fig. 1. Simulation model of the communication system.

TABLE I
LTE DOWNLINK PHYSICAL LAYER PARAMETERS

Parameter	Value
Bandwidth	20 MHz
FFT size	2048
Number of data subcarriers	1200 (dc[1] subcarrier not included)
FEC	Turbo code
Coding rate	1/3
Modulation scheme	64QAM

[1]Direct current.

II. SYSTEM ASSUMPTIONS

In the following, we use the 3GPP LTE (4G) standard as an illustrative example for the analysis of the interference impact on OFDM systems.

A. System Model

In OFDM, each subcarrier carries a separate stream of information, causing information to be mapped into both the time and the frequency domains. This gives an OFDM time-frequency lattice, which is a two-dimensional grid used to represent how information is mapped to both the subcarrier and the OFDM symbol.

The LTE system that is based on OFDM operates with 1200 subcarriers carrying the information. In this work, we investigate how the interference affects the system performance when one or all of the 1200 subcarriers are subjected to narrowband interference. The work focuses on examining how a narrowband interference on one subcarrier, in general, affects the orthogonality in the OFDM system. Furthermore, we consider the case when the interfering signal consists of several narrowband signals. In addition, the impact from broadband AWGN is studied.

In our simulation model, the interference is added on the radio channel time representation of the OFDM signal. The system performance is analyzed in terms of BEP. There are also other available performance measures to quantify the communication performance. In this work, the BEP is chosen as a suitable performance measure, since it is a general measure from which packet or frame error probability and throughput can be estimated. Furthermore, the BEP is not dependent on higher layer mechanisms and particular applications. In a real LTE system, some of the subcarriers are used for vital reference and synchronization signals [20]. Hence, if such a signal is subjected to interference, this will cause system effects worse than only bit errors on an arbitrary channel [8]–[12]. We will not consider such system effects in our analyses, which means that the BEP shown in our results can be seen as lower bound from a certain system point of view.

The simulation model is shown in Fig. 1. The simulation starts by creating the data information as random bits and thereafter applies the forward error correction code (FEC) turbo encoding. The turbo encoder is a parallel concatenated convolutional code with two 8-state constituent encoders and a turbo code internal interleaver. The coding rate of the turbo code is 1/3. Next, the data stream is mapped to predefined constellations points, dependent on the used modulation scheme, into the subcarriers. For all subcarriers, the used modulation scheme is 64-quadrature amplitude modulation (64-QAM). At this point, in a real system, the pilot carriers would also be inserted. After the inverse FFT, the interference is added to the transmitted OFDM time signal. This is done in the block radio channel, see Fig. 1. The interference signals are further described in Section II-B. The FFT is performed on the received signal and after demodulation, the turbo decoding (FEC) is applied on soft decision bits from the demodulator to retrieve the information bits. After the channel decoding (FEC decoding), the BEP is estimated by comparing the original bit sequence with the received sequence. The BEP is then calculated as the ratio between the number of incorrect received bits and the total number of received information bits. The BEP curves are achieved by generating the BEP for a varying signal-to-interference ratio (SIR). The SIR is defined as E_b/N_I, where E_b is the energy per data bit and N_I is the interference power spectral density [W/Hz].

In all simulations, we assume perfect time synchronization of the OFDM signal and, therefore, there is no need of a cyclic prefix to handle this. In our analysis, we, therefore, assume that we have a standard OFDM system that handles ISI. Since the CW interference does not introduce extra ISI (since the CW power is only spread within the subcarriers of one OFDM-symbol), we do not need to analyze this in our case. Hence, the simulation model does not include the effects from ISI. In the simulations, LTE parameters in Table I are used.

B. Interference Signal Model

The radio channel interference is assumed to be either AWGN or consist of one or many CW signals. In order to focus on the effects from the CW interference, perfect timing, phase, and frequency synchronization are assumed. For this type of signal, the received time-domain signal is given by

$$r(n) = s(n) + i(n) \tag{1}$$

where $s(n)$is the OFDM signal with samples $n = 1, \ldots, N_{\mathrm{FFT}}$, and N_{FFT} is the FFT size. The interfering signal $i(n)$consists of either a single CW $i_{\mathrm{CW}}(n)$, many CW signals $i_{N_{\mathrm{CW}}}(n)$, or broadband AWGN interference $i_{\mathrm{AWGN}}(n)$ over the system bandwidth, with zero-mean and variance equal to σ^2. For all the interference alternatives, the interference power is assumed to be equal. This means that the single CW has all the interference power on one frequency, whereas for the case with several CW

signals or for broadband AWGN, the same amount of interference power is distributed over the whole system bandwidth. The single CW $i_{\mathrm{CW}}(n)$ is modeled as a complex exponential signal

$$i_{\mathrm{CW}}(n) = \sqrt{\frac{P_{\mathrm{I}}}{N_{\mathrm{FFT}}}} e^{j\left(\frac{2\pi}{N_{\mathrm{FFT}}}(m+\alpha)n+\theta\right)} \tag{2}$$

where P_I is the interference power, m is the subcarrier closest to the CW frequency, and θ denotes a uniformly distributed random phase $\theta \sim U[-\pi, \pi]$. The interference power P_I is related to N_I as $P_I = N_I B$, where N_I is the average single-sided spectral density power and B is the subcarrier bandwidth, assuming AWGN. Furthermore, α is the frequency separation between the CW signal and subcarrier m. The frequency of the CW is selected to be the same as one of the subcarrier frequencies or somewhere between two adjacent subcarriers, while α typically assumes values as $\alpha \in [-0.5, 0.5]$. Note that for $\alpha = 0$, the CW signal is located directly on one of the subcarriers and is, therefore, orthogonal to the other subcarriers. For the case when the interference consist of N_{CW} CW signals, all are assumed to have different frequencies, and the new signal can be described as

$$i_{N_{\mathrm{CW}}}(n) = \sqrt{\frac{P_{\mathrm{I}}}{N_{\mathrm{FFT}} N_{\mathrm{CW}}}} \sum_{p=1}^{N_{\mathrm{CW}}} e^{j\left(\frac{2\pi}{N_{\mathrm{FFT}}}(m_p+\alpha)n+\theta_p\right)} \tag{3}$$

with the CW signal number $p = 1, \ldots, N_{\mathrm{CW}}$. If the CW signals are assumed to be synchronized, their phases θ_p are all the same. Also, their amplitudes are equally set to $\sqrt{P_I/N_{\mathrm{CW}}}$. The interference case with several CW signals is here defined as (3), with $N_{\mathrm{CW}} = 1200$ and $N_{\mathrm{FFT}} = 2048$, equal to the OFDM system.

On the receiver side, after taking an N_{FFT} point FFT on $i_{\mathrm{CW}}(n)$ in (2), the narrowband interference frequency representation on subcarrier k is given by [3]

$$I_{k,\mathrm{CW}} = \sqrt{\frac{P_I}{N_{\mathrm{FFT}}}} e^{j\theta} \frac{1 - e^{j2\pi\alpha}}{1 - e^{j\frac{2\pi}{N_{\mathrm{FFT}}}(m-k+\alpha)}}. \tag{4}$$

When the interference is located at a subcarrier m, i.e., for $\alpha = 0$, the interference only affects the subcarrier m and (4) reduces to [2]

$$I_{k,\mathrm{CW}} = \begin{cases} \sqrt{P_{\mathrm{I}} N_{\mathrm{FFT}}} e^{j\theta}, & k = m \\ 0, & k \neq m \end{cases}. \tag{5}$$

The case where the interference consists of several CW signals is treated in the same manner.

Due to the composition and the frequency spacing of the subcarriers, the subcarriers are orthogonal to each other. This is a fundamental property of OFDM. If a CW signal is located at a subcarrier frequency, the interference will only affect the same subcarrier and no other subcarrier. This is evident in (5), where it can be seen that the interference power due to the CW signal, when $\alpha = 0$, only appears at that subcarrier in the demodulation. However, if the CW signal is located at another frequency, i.e., somewhere between subcarriers, the orthogonality in the OFDM signal is violated and the interference will affect several subcarriers in the demodulation. As can be seen from (4), $I_{k,\mathrm{CW}} \neq 0$, if $\alpha \neq 0$ regardless if $k = m$ or $k \neq m$. This can also be understood by noting that the FFT of a single narrowband signal, with $\alpha \neq 0$, will give a wide spectral content.

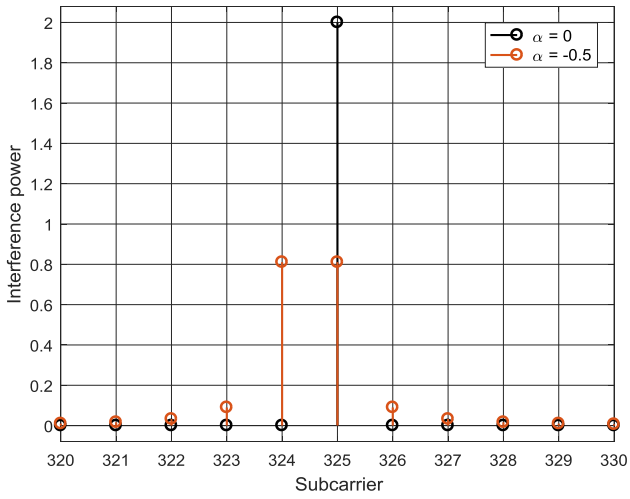

Fig. 2. Interference power distribution after the FFT when the OFDM system is subjected to one CW signal (closest to subcarrier $m = 325$), with separation $\alpha = 0$ and -0.5 from the subcarrier 325.

There is, however, one situation when the system may have difficulties when the CW signal is located exactly at a subcarrier. As mentioned earlier, some of the subcarriers are usually allocated as reference signals, as they are called in the 3GPP technical specifications [20]. The information obtained from the reference signals is used by the receiver for channel estimation. The location and use of such signals are system dependent. Since the reference signals handle the channel estimation among the subcarriers around the reference signal, interference to a reference signal will affect the data transmission of those subcarriers that the reference signal supports. Those kinds of effects are, however, not analyzed in this work.

III. Simulation Results

As indicated in the previous section, the position of an interfering CW signal may be crucial, since its power may be spread to several OFDM subcarriers. The effects of this will be analyzed in terms of BEP for different kinds of interference waveforms and comparisons are made with AWGN. In particular, the difference in E_b/N_I will be studied for a BEP requirement of 10^5. The difference in E_b/N_I shows if the system is more sensitive to certain interference waveforms. It should be noted that the current emission requirements do not consider the interference waveform and in many measurements only the rms value is captured. Fig. 2 shows an example of how the interference power is spread to different subcarriers after the FFT in the receiver for $\alpha = 0$ and -0.5. The results in the figure are obtained by simulations of the communication system, see Fig. 1, but can also be calculated by using (4). The power is normalized for comparison between the two values of α. For $\alpha = 0$, only the subjected subcarrier is affected by interference power, whereas for $\alpha = -0.5$, the interference power is distributed on several subcarriers. Highest interference power will occur at the two closest subcarriers and then the interference power will diminish as we go further away from these two subcarriers.

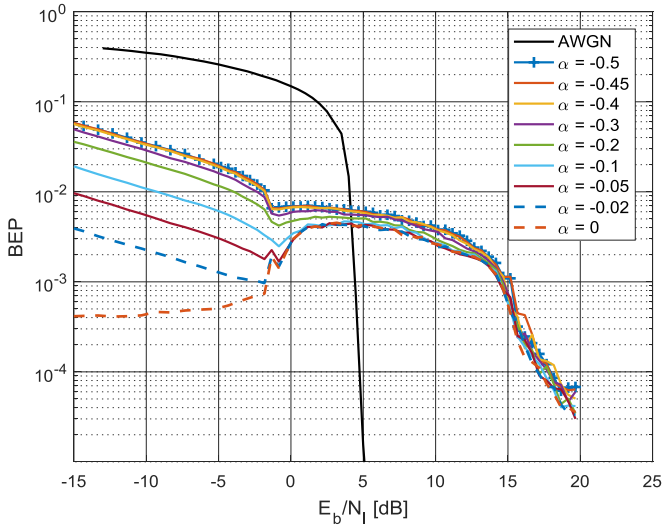

Fig. 3. BEP as a function of E_b/N_I when the system is subjected to a CW signal α from a subcarrier.

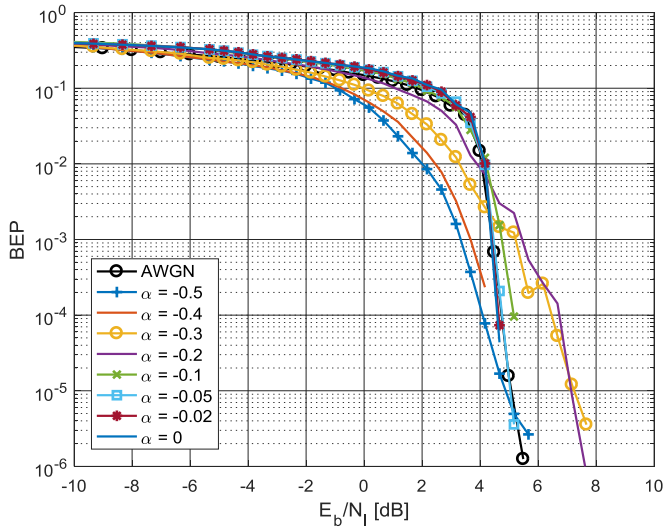

Fig. 4. BEP as a function of E_b/N_I when the system is subjected to several synchronously CW signals, with the frequency deviation α from the subcarriers.

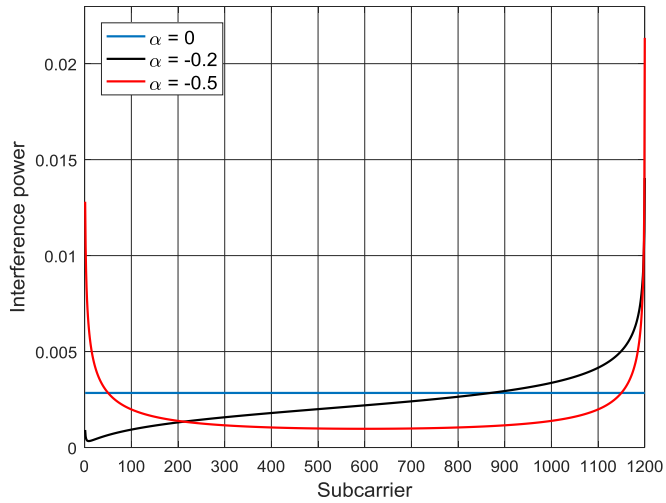

Fig. 5. Interference power distribution over the data subcarriers after the FFT when the OFDM system is subjected to several synchronously CW signal, $\alpha = -0, -0.2$, and -0.5 from the subcarriers.

In Fig. 3, the BEP is simulated for different E_b/N_I for a coded system with similar parameters as the LTE system. In the simulation, it is assumed that the CW signal is located either at a subcarrier or between two subcarriers, here varied by the value of α. For E_b/N_I less than –1 dB, there is a substantial difference in impact depending on where in frequency the CW is located. The largest impact occurs when the CW signal is located exactly between two subcarriers, i.e., when $\alpha = -0.5$. When $E_b/N_I > -1$ dB, the difference vanishes. In addition, for $E_b/N_I > -1$ dB and up to $E_b/N_I = 5$ dB, the BEP in fact gets worse. This is due to the difficulties the Turbo decoder faces due to a varying interference power when estimating the interference power in the decoding process. The decoder continuously estimates the interference power. This behavior is observed in [13] and [14].

When the OFDM system is subjected to a CW signal, the interference behaves as an impulsive interference to a single carrier system when the signal enters the decoder. This is further explained in the Appendix. Furthermore, a threshold effect and a noise probability density function mismatch may appear in the decoder, since the decoder is optimized to AWGN [15]. The figure also shows that AWGN causes larger degradation than the CW signal for $E_b/N_I < 5$ dB. For larger E_b/N_I, the CW interference is considerably worse than AWGN. For a BEP of 10^5, which is a BEP requirement commonly used for data transmission, the difference in E_b/N_I between AWGN and CW is about 18 dB.

This means that the communication system is more sensitive to a CW interference and that a CW interference needs to be 18 dB lower in interference power to yield the same BEP (BEP $= 10^5$) as AWGN.

For the case when the interference consists of several interfering CW signals, the impact on the OFDM system is very different. The behavior is even different between synchronous and nonsynchronous CW signals. In Fig. 4, the BEP is shown for several synchronously CW signals and different α, as well as for AWGN. The synchronized CW signals are all assumed to have the same phase. Later, also unsynchronized CW signals are studied. For that case, each CW signal is assumed to have a random phase independent of each other and independent of the OFDM system. The case with synchronized CW signals does not constitute a relevant real case and is only included as a comparison to the unsynchronized case.

The BEP curves in Fig. 4 are close to AWGN performance for all α. Furthermore, again it is shown that the BEP depends on the frequency deviation α from the subcarriers, but in a different way than in Fig. 3, and not at all as much as for one CW signal. The performance for $\alpha = -0.5$ represents, in contrast to the case shown in Fig. 3, the lowest BEP. The worst degradation is experienced by $\alpha = -0.2$ and -0.3 for large E_b/N_I.

Fig. 5 shows the distribution of interference power after the FFT when the interference consists of synchronized CW signals located at $\alpha = 0, -0.2$, or -0.5. For the values of α, the interference power is varying at the subcarriers. The symbols that enter the decoder are retrieved sequentially from the subcarriers, and the decoder will experience a varying interference power

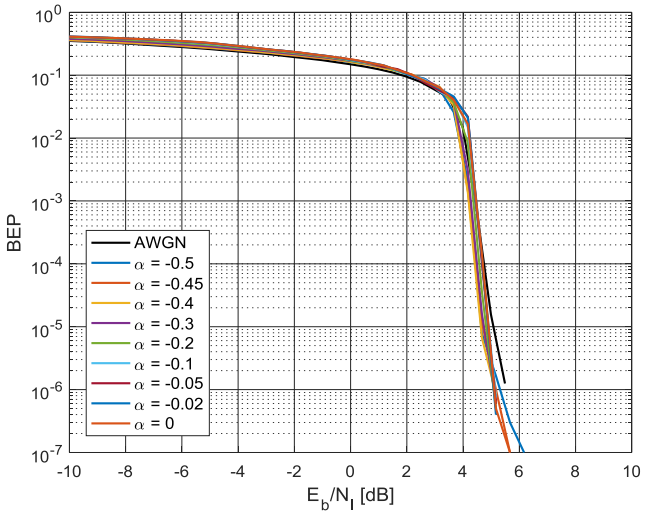

Fig. 6. BEP as a function of E_b/N_I when the system is subjected to several unsynchronized CW signal α from the subcarriers.

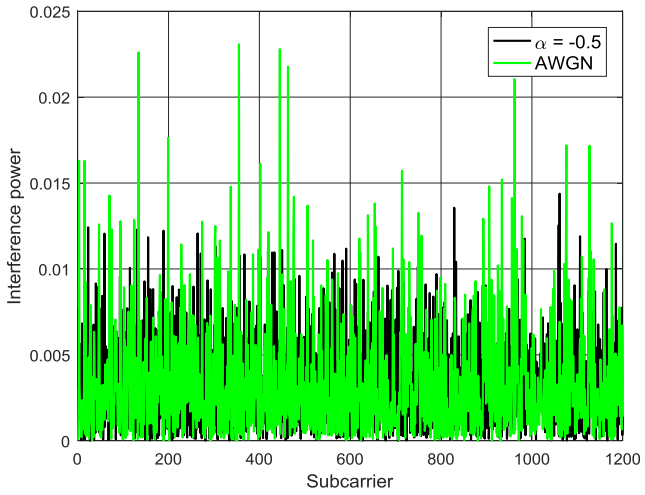

Fig. 7. Interference power distribution over all the subcarriers after the FFT when the OFDM system is subjected to several unsynchronized CW signal, with the separation $\alpha = -0.5$ from the subcarriers or broadband AWGN with equal average power, to compare with.

over time (see the Appendix). For $\alpha = 0$, the demodulated CW signals create a constant level of the interference power on each subcarrier. Hence, the impact becomes very similar to a system subjected to AWGN. For nonzero values of α, the interference power is varying at the different subcarriers, which results in a lower slope of the BEP curve than for AWGN and for $\alpha = 0$.

For the situation when the interference consists of several interfering unsynchronized CW signals, the BEP is rather similar to the case when the system is disturbed by AWGN. When the interfering signals are unsynchronized, the BEP no longer depends on α. The BEP for several interfering unsynchronized CW signals is very similar to the BEP for AWGN, see Fig. 6. As the phase values of the interfering CW signals are random, the interference power distribution over the subcarriers after the FFT appears as random too, see Fig. 7, which is very similar to AWGN.

Altogether, the impact is reduced as the number of CW signals gets larger and they become unsynchronized to each other

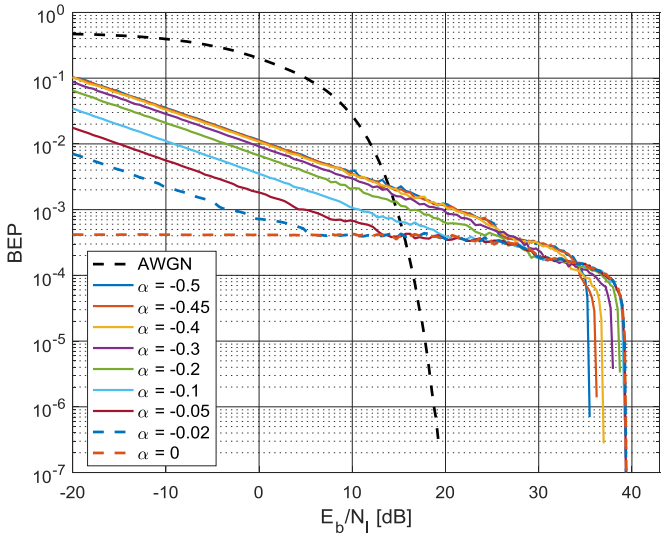

Fig. 8. BEP as a function of E_b/N_I for an uncoded system (hard decision, 64-QAM) subjected to a CW signal α from a subcarrier.

while maintaining the same interference power. This depends on how the FFT in the OFDM receiver treats the interference signal in combination with the Turbo decoder. If the system is not utilizing any coding at all, the degradation becomes severe. In Fig. 8, the BEP is shown for an uncoded system that is subjected to one CW signal. The demodulator is for this case delivering hard decisions. Here, it is particularly evident that the interference after the FFT appears as an impulsive interference to the Turbo decoder and differs substantially from the case with AWGN. The BEP curves get the characteristic behavior of impulsive interference with a clear plateau at an approximate level of $1/(2N_{\mathrm{CW}})$ for low E_b/N_I and a much worse degradation than for AWGN for high E_b/N_I. For a BEP of 10^5, the difference in E_b/N_I between AWGN and CW is about 18 dB.

If the interfering signal consists of several unsynchronized CW signals, see Fig. 9, the BEP curves get a totally different behavior and the impact becomes much less than for AWGN in a large region of E_b/N_I. Least degradation is obtained by $\alpha = 0$. For $\alpha = 0$, the interference power is spread over the subcarriers after the FFT with a constant level in average. As α increases, the interference power variation among the subcarriers after the FFT also increases, and the degradation becomes worse. This is similar to a single-channel system that is subjected to fading, where the degradation gets worse as the fading increases.

From the above-mentioned results, we can draw the following conclusions. For both coded and uncoded systems

1) a single CW signal results in a substantially worse impact than several CW signals or broadband AWGN for larger E_b/N_I (or BEP $< 10^3$). For BEP $= 10^5$, the difference in E_b/N_I between AWGN and a single CW is about 18 dB.
2) the impact of interfering CW signals may be largely dependent on the frequency position α.

IV. Discussion

In standard radiated emission limits, the resolution bandwidth is defined for different frequency bands [16], [17]. In Table II, examples of such bandwidths are shown for some common

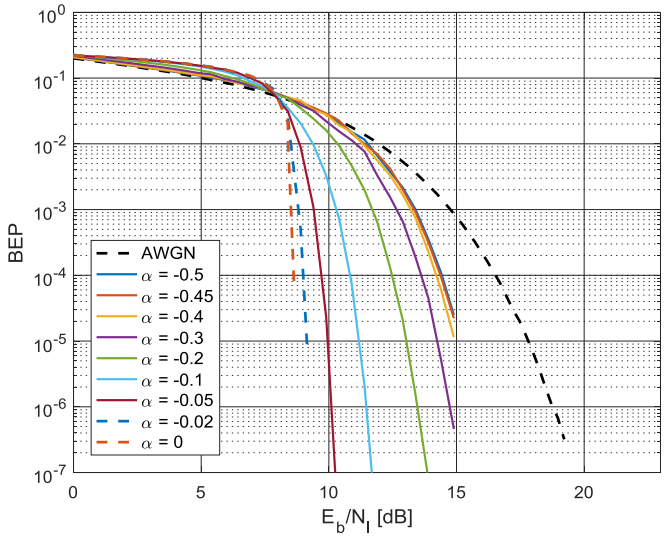

Fig. 9. BEP as a function of E_b/N_I for an uncoded system (hard decision, 64-QAM) subjected to several unsynchronized CW signals, with varying α from a subcarrier.

TABLE II
EXAMPLES OF RESOLUTION BANDWIDTH FOR DIFFERENT CIVILIAN RADIATED EMISSION STANDARDS [16], [17]

Standard/frequency band	Resolution bandwidth
EN 55022	
30–1000 MHz	120 kHz
1–18 GHz	1 MHz
FCC Part 15 Subpart B	
150 kHz to 30 MHz	9 kHz
30–1000 MHz	120 kHz
1–40 GHz	1 MHz

civilian standards. No difference of the limits is made between wideband and narrowband emissions. This means that the same limit is set whether the interference is, for example, wideband noise or a single sinusoidal CW signal. For many communication systems, this does not cause any problems with respect to the relation between emission limit and interference impact on a digital communication receiver. For example, in a 3G UMTS receiver, a strong CW signal will be spread by the spreading code so that the interference impact will be approximately equal to a wideband interference signal with the same average power within the measurement bandwidth [18]. Also for digital communication systems using typical digital modulation schemes, the fact that wideband noise is measured with the same bandwidth as a CW signal will not cause any major problem with respect to the interference impact [19]. However, for OFDM, where the modulation scheme is built up by narrowband subchannels, this is not true. For OFDM, it is a problem that radiated emission limits use the same bandwidths independent of the interference waveform. Since it has been shown that CW interference can have significant performance degradation on OFDM systems, the interference level has to be considered in the determination of maximum allowed emission levels. Furthermore, since CW interference can have a large impact on

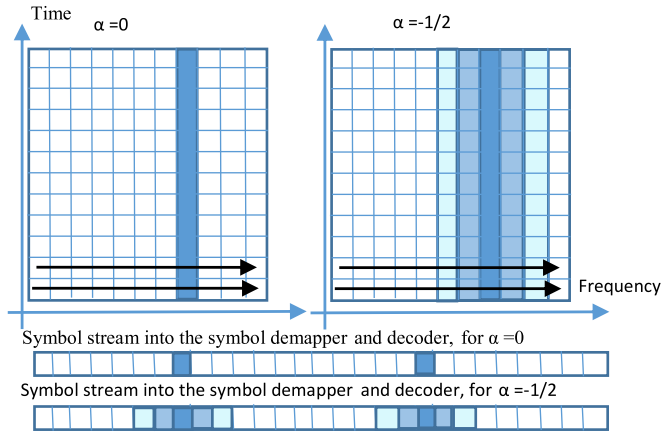

Fig. 10. Frequency–time grid of an OFDM system and an interfering CW signal at one subcarrier $\alpha = 0$ or in the between of two subcarriers $\alpha = -0.5$.

several adjacent subcarriers, it is reasonable to adjust the maximum allowed CW interference by considering the bandwidth W_{SC} of the subcarrier. W_{SC} is typically in the order of some tens of kHz, while the measurement bandwidth W_M is typically in the region of hundreds of kHz up to 1 MHz, depending on the frequency region. A reasonable adjustment of the maximum allowed CW-interference level is, therefore, by decreasing the level by a scaling with W_M/W_{SC}. For example, with a measurement bandwidth of 1 MHz and a subcarrier bandwidth of 15 kHz, the emission level could be adjusted with the factor $\sqrt{15 \cdot 10^3/1 \cdot 10^6}$ corresponding to about –18 dB. This means that the permitted emission limit for the CW interference is reduced by 18 dB. This corresponds very well with the result for the coded and the uncoded case in Figs. 3 and 8, respectively, for a BEP of 10^5.

V. CONCLUSION

The presented results show that by varying the CW interference between single subcarriers in an OFDM-based system, the resulting BEP can vary within several magnitudes. Furthermore, for both coded and uncoded systems, a single CW signal constitutes substantially worse impact than several CW signals or broadband AWGN in the region where BEP $< 10^3$. Thus, an OFDM system is considerably more sensitive for a single CW than AWGN interference or several CW signals. As an example, the power of a CW interference within a single subcarrier, at a BEP of 10^5, is about 18 dB lower than the corresponding power of AWGN interference.

Since OFDM-based systems are used in a large variety of wireless systems, this vulnerability should be considered in emission measurements. A further development of present radiated emission standards is needed to handle this problem and we have highlighted some important issues in this work. However, further work is needed to find a convenient solution to this problem for future radiated emission standards.

APPENDIX

In Fig. 10, the frequency–time grid of an OFDM system is depicted. When a single CW signal is located at a subcarrier,

$\alpha = 0$, or between two subcarriers $\alpha = -0.5$, the interference power after the FFT is either not spread at all or spread to the adjacent subcarriers. QAM symbols are retrieved by the QAM demodulator in parallel at the different subcarriers. The QAM symbols are then transformed into a serial sequence and enter the symbol demapper and the decoder. The figure shows that the interference will be spread between the symbols in different ways depending on the value of α.

REFERENCES

[1] A. Goldsmith, *Wireless Communications*. Cambridge, U.K.: Cambridge Univ. Press, 2009.

[2] A. Batra and J. R. Zeidler, "Narrowband interference mitigation in OFDM systems," in *Proc. IEEE Mil. Commun. Conf.*, San Diego, CA, USA, Nov. 2008, pp. 1–7.

[3] P. Ankarson, J. Carlsson, B. Bergqvist, S. Larsson, and M. Bertilsson, "Impact of different interference types on an LTE communication link using conducted measurements," in *Proc. IEEE Int. Symp. Electromagn. Compat.*, Dresden, Germany, Aug. 2015, pp. 177–182.

[4] P. F. Stenumgaard, "A simple method to estimate the impact of different emission standards on digital radio receiver performance," *IEEE Trans. Electromagn. Compat.*, vol. 39, no. 4, pp. 365–371, Nov. 1997.

[5] F. Sabath, "Threat of electromagnetic terrorism—Lessons learned from documented IEMI attacks," in *Proc. EUROEM*, Toulouse, France, Jul. 2012.

[6] R. R. Tanuhardja, S. van de Beek, M. J. Bentum, and F. B. J. Leferink, "Vulnerability of terrestrial-trunked radio to intelligent intentional electromagnetic interference," *IEEE Trans. Electromagn. Compat.*, vol. 57, no. 3, pp. 454–460, Jun. 2015.

[7] D. Månsson, R. Thottappillil, M. Bäckström, and O. Lundén, "Vulnerability of European rail traffic management system to radiated intentional EMI pulses," *IEEE Trans. Electromagn. Compat.*, vol. 50, no. 1, pp. 101–109, Feb. 2008.

[8] M. Lichtman, J. H. Reed, T. C. Clancy, and M. Norton, "Vulnerability of LTE to hostile interference," in *Proc. IEEE Global Conf. Signal Inf. Process.*, Dec. 2013, pp. 285–288.

[9] P. Stenumgaard, K. Fors, and K. Wiklundh, "Interference impact on LTE from radiated emission limits," in *Proc. 2015 IEEE Int. Symp. Electromagn. Compat.*, Dresden, Germany, Aug. 2015, pp. 165–170.

[10] T. C. Clancy, M. Norton, and M. Lichtman, "Security challenges with LTE-advanced systems and military spectrum," in *Proc. Mil. Commun. Conf.*, Nov. 2013, pp. 375–381.

[11] R. P. Jover, J. Lackey, and A. Raghavan, "Enhancing the security of LTE networks against jamming attacks", *EURASIP J. Inf. Secur.*, vol. 2014, Apr. 2014, Art. no. 7.

[12] G. Philippe *et al.*, "LTE resistance to jamming capability: To which extend a standard LTE system is Able to resist to intentional jammers," in *Proc. Mil. Commun. Inf. Syst. Conf.*, Oct. 2013, pp. 1–4.

[13] P. C. Hsian and P. C. Chin, "Evaluation of variance mismatch for serial turbo codes with Talwar penalty function under interference of impulsive noise," *J. Eng. Sci. Technol.*, vol. 5, no. 3, pp. 350–360, 2010.

[14] D. Umehara, M. Kawai, and Y. Morihiro, "A suboptimal receiver for PCSS system over class a noise channel," in *Proc. Int. Symp. Inf. Theory Appl.*, Xi'an, China, Oct. 2002.

[15] T. Shongwe, A. J. Han Vinck, and H. C. Ferreira, "The effects of periodic impulsive noise on OFDM," in *Proc. IEEE Int. Symp. Power Line Commun. Appl.*, Austin, TX, USA, Mar. 2015, pp. 189–194.

[16] FCC Part 15 Subpart B, 2010.

[17] *Information Technology Equipment–-Radio Disturbance Characteristics–-Limits and Methods of Measurement*, EN 55022:2010, 2010.

[18] M. K. Simon, J. K. Omura, R. A. Scholtz, and B. K. Levitt, *Spread Spectrum Communications*, vol. II. New York, NY, USA: Comput. Sci. Press, 1985.

[19] K. Wiklundh, "Impact of some interfering signals on a MSK receiver under fading conditions," in *Proc. 21st Century Mil. Commun. Archit. Technol. Inf. Superiority (Cat. No.00CH37155)*, Los Angeles, CA, USA, Oct. 2000, pp. 377–381.

[20] ETSI TS 136 211, LTE; Evolved Universal Terrestrial Radio Access (E-UTRA); Physical channels and modulation (3GPP TS 36.211 version 10.0.0 Release 10).

Karina Mariana Fors received the B.Sc. and M.Sc. degrees in electrical engineering from Linköping University, Linköping, Sweden, in 2001 and 2006, respectively.

Since 2001, she has been working with the Swedish Defence Research Agency (FOI), Linköping, Sweden. She is currently a Senior Scientist with FOI. Her main research interests include intersystem interference and analyzing methods used to estimate the interference impact on radio communication systems. Other topics of research interest include channel modeling for wireless communications, submarine communication, and signal detection methods used to discriminate different interference signals.

Kia Cecilia Wiklundh was born in 1968. She received the Master of Science degree in electrical engineering from Linköping University, Linköping, Sweden, in 1995, and the Ph.D. degree in the area of interference impact on radio communication systems from Chalmers University of Technology, Göteborg, Sweden, in 2007.

In 1995, she joined the Department of Information Systems, Swedish Defence Research Agency (FOI), Linköping, Sweden. Since then, she has worked in the field of robust radio communication systems both for the Swedish military forces and for civilian customers. She is currently a Deputy Research Director with FOI and works both with research and project management. Her special field is intersystem interference, and she has worked with a variety of areas, for example, with submarine communication and high capacity data links for airplanes. Other topics of research interests include electromagnetic compatibility, modulation and coding techniques especially for non-Gaussian noise, multiple-input multiple-output, and communication theory.

Dr. Wiklundh is currently the Chair of Section E (The Electromagnetic Environment and Interference Commission) of the Swedish National Committee of URSI and the Vice Chair of the EMC Chapter of the IEEE Sweden. She was the recipient of three awards for her scientific work.

Peter F. Stenumgaard received the Ph.D. degree in radio communications from the Royal Institute of Technology, Stockholm, Sweden, in 2001.

Since 1995, he has been working with the Swedish Defence Research Agency (FOI), Linköping, Sweden. He is a Research Director in Robust Telecommunications and works currently as the Head with the Department of Information Security & IT Architecture, FOI. He has worked as an Adjunct Professor, both with the Department of Communication Systems, Linkoping University (2011–2014) and with the Radio Center, University of Gavle (2007–2012). He has long experience of research on interference issues for critical wireless applications in military and civilian communications. He has also been the Director of the Graduate School Forum Securitatis (2010–2014), Linköping University, within Security and Crisis Management. In 1989–1995, he worked for several years on the JAS fighter aircraft program, on the protection of aircraft systems against electromagnetic interference, lightning, nuclear weapon generated electromagnetic pulse, and high-power microwaves. He has a total of some hundred scientific journal and conference publications.